The effect of surface roughness on the determination of optical constants of CuInSe2 and CuGaSe2 thin films

G. Yin, C. Merschjann, and M. Schmid

Articles you may be interested in

Properties of Cu(In,Ga,Al)Se2 thin films fabricated by magnetron sputtering
J. Vac. Sci. Technol. A **33**, 031201 (2015); 10.1116/1.4913863

Strength, stiffness, and microstructure of Cu(In,Ga)Se2 thin films deposited via sputtering and co-evaporation
Appl. Phys. Lett. **105**, 011907 (2014); 10.1063/1.4890086

Morphology and structure evolution of Cu(In,Ga)S2 films deposited by reactive magnetron co-sputtering with electron cyclotron resonance plasma assistance
J. Appl. Phys. **115**, 084902 (2014); 10.1063/1.4866717

Insights on the influence of surface roughness on photovoltaic properties of state of the art copper indium gallium diselenide thin films solar cells
J. Appl. Phys. **111**, 114509 (2012); 10.1063/1.4721648

Determination of Mass Attenuation Coefficients for CuInSe2 and CuGaSe2 Semiconductors
AIP Conf. Proc. **899**, 169 (2007); 10.1063/1.2733090

The effect of surface roughness on the determination of optical constants of CuInSe$_2$ and CuGaSe$_2$ thin films

G. Yin,[1,a)] C. Merschjann,[2,3] and M. Schmid[1]

[1]*Helmholtz-Zentrum Berlin für Materialien und Energie, Nano-optical Concepts for PV, Hahn-Meitner-Platz 1, 14109 Berlin, Germany*
[2]*Helmholtz-Zentrum Berlin für Materialien und Energie, Heterogeneous Material Systems, Hahn-Meitner-Platz 1, 14109 Berlin, Germany*
[3]*Universität Rostock, Institut für Physik, Universitätsplatz 3, 18051 Rostock, Germany*

To investigate the effect of surface roughness on the calculation of optical constants, e.g., the complex refractive index $n + ik$ or (n, k) of CuIn$_{1-x}$Ga$_x$Se$_2$ (CIGSe) thin films, we took CuInSe$_2$ (CISe) and CuGaSe$_2$ (CGSe) as examples and applied the "Modified Transfer-Matrix (MTM)" method to calculate optical constants with considering the effect of scattering due to surface roughness. Compared to the Transfer-Matrix (TM) method without considering surface roughness, it was revealed that the MTM method could improve the accuracy of calculation. The calculated refractive index values from the MTM method increase by 6.89% for CISe and 2.59% for CGSe in contrast to those from the TM method. In addition, bromine solution was confirmed via Scanning Electron Microscopy and Atomic Force Microscopy to be able to reduce the surface roughness. Calculated results from smoothened samples showed that the accuracy of calculated optical constants was further improved. Finally, optical constants calculated by the MTM method were compared to those from smoothened samples, validating that the MTM method could eliminate the influence of surface roughness on the calculation of optical constants more effectively for CGSe with low surface roughness than for CISe with high surface roughness. © *2013 AIP Publishing LLC*. [http://dx.doi.org/10.1063/1.4809550]

I. INTRODUCTION

The application of polycrystalline chalcopyrite CuIn$_{1-x}$Ga$_x$Se$_2$ (CIGSe) thin films for solar cells has been extensively investigated since the early 1980s (Ref. 1) and an efficiency beyond 20% has been proven on lab scale.[2] The optical constants (complex refractive index $n + ik$ or (n, k)) of each film in the CIGSe solar cell are the basic parameters for quantitative calculation of the absorption profile. They thereby provide the potential to optimize the structure optically, such as reducing the reflectance and minimizing the thickness of the absorber layer,[3] which is especially important for the ultra-thin and transparent solar cells.[4] In the stacked-layer structure of a CIGSe solar cell, the CIGSe film serves as the absorber and plays the most important role in the solar cell. To achieve the goal of simulating this layer, accurate optical constants of CIGSe thin films are highly desirable.

Although optical constants of CIGSe compounds have already been studied in the past for bulk materials as well as for thin films,[3,5–8] the influence of surface roughness was not considered specifically in most cases. But we will see that the surface roughness can play a significant role in the investigation of optical constants. It is thus of high importance and necessity to re-investigate the optical constants considering the influence of surface roughness.

The optical constants of solids can, in principle, be obtained by either polarimetric or photometric methods. In this paper, we focus on macroscopic T/R measurements related to the class of photometric methods. From the measured T/R, we apply the Fresnel coefficients-based Transfer-Matrix (TM) method[3,9] to calculate the optical constants of the thin films. This approach is widely used for its simplicity[10] and the same illumination geometry as in the solar cell.[3] It can deal with both coherent propagation of light through smooth thin films and incoherent propagation through thick substrates. However, CIGSe films usually exhibit relatively high surface roughness,[11,12] which can lead to scattering (partially coherent propagation) within the films and results in substantial intensity reduction of reflectance (R) and transmittance (T) especially at short wavelengths.[13] To consider the roughness and overcome this difficulty, we introduce modified Fresnel coefficients into the TM method (MTM) compensating for the loss of measured R/T of real films due to the surface roughness and correlate measured R/T to the corresponding calculated parts for the same, but perfectly smooth surface.[14] The MTM method has been applied to investigate the influence of surface and interface roughness on R/T.[15,16] We will apply the MTM method inversely to calculate the optical constants and study how the method affects the calculation of optical constants.

In this work, CuInSe$_2$ (CISe) and CuGaSe$_2$ (CGSe) films were taken to obtain experimental data. Optical constants of CISe and CGSe were calculated with and without surface roughness consideration. In addition, CISe and CGSe films were smoothened with bromine solution and the according calculated optical constants were compared to those obtained by the MTM method.

a)Email: guanchao.yin@helmholtz-berlin.de

II. EXPERIMENTAL DETAILS

A. Sample preparation, surface roughness determination, and optical measurements

CISe and CGSe films were deposited onto microscope slides via the standard 3-stage co-evaporation process[2] at a substrate temperature of 610 °C. The original thickness ranges from 300 to 400 nm. Aqueous bromine solution was shown to be able to reduce the surface roughness of CISe and CGSe.[17] In this work, the bromine was diluted with water with a concentration of 0.02 mol/l. The whole smoothening process was performed at room temperature: the samples were submerged in the bromine solution for 4 min and then rinsed with distilled water and pure ethanol, finally dried with N_2 for further measurements. KCN etching was then done to remove the residual Se on the surface.[17] Scanning Electron Microscopy (SEM) and Atomic Force Microscopy (AFM) were used to determine the surface roughness of the films before and after smoothening. Optical measurements were carried out using an UV-Vis spectrophotometer with an integrating sphere, which enables to measure total transmittance (T_{tot}), total reflectance (R_{tot}), and its diffuse parts. Then the specular transmittance (T_{spe}) and specular reflectance (R_{spe}) can be calculated by subtracting the diffuse from the total part.

B. Calculation of optical constants

The TM method allows to obtain analytical expressions of transmittance (T_{cal}) and reflectance (R_{cal}) of a layer stack as a function of optical constants and thickness of each layer. By comparing the analytical expressions to the measured R/T, parameters like optical constants can, in principle, be determined. The TM method assumes that each layer is optically homogenous and isotropic, and the interface between layers is smooth. Fig. 1 illustrates the layer-stacking structure of the samples in our experiment. The structure is composed of 4 media: air (a)/a thin layer (b)/an optically thick layer (c)/air (d) and is under normal incidence of light from the thin film (CIGSe) side. The thicknesses of the CIGSe film (medium b) and the substrate (medium c) can be measured; the optical constants of the substrate (n_c, k_c) and of air ($N_a = N_d = 1$) are known. Then two implicit equations (Eqs. (1) and (2)) can be determined by the TM method with variables of optical constants of CIGSe (n_b, k_b) for each wavelength[3]

$$R_{cal}(n_b(\lambda), k_b(\lambda)) - R_{tot}(\lambda) = 0, \tag{1}$$

$$T_{cal}(n_b(\lambda), k_b(\lambda)) - T_{tot}(\lambda) = 0. \tag{2}$$

Here, λ is the wavelength. For flat interfaces, $R_{tot}(\lambda)$ and $T_{tot}(\lambda)$ are equal to the specular parts $R_{spe}(\lambda)$ and $T_{spe}(\lambda)$, respectively. In principle, $n_b(\lambda), k_b(\lambda)$ can be solved based on the Eqs. (1) and (2). However, multiple solutions exist due to the implicit nature of the two equations.

In the following, we will illustrate how to obtain the analytical expressions for T_{cal} and R_{cal} based on the TM method.

1. TM method

The TM method has been investigated in detail to calculate the R/T for a stacked structure.[18,19] In the following, we will present how the TM method works for the sample structure in our work. In Fig. 1, at each interface in this layer stack, one part of the incident light will be transmitted to the adjacent medium and the other part reflected. Thereby the electric field of the electromagnetic wave in each medium is divided into two parts: the forward component E^+ and the backward component E^-. The electric field amplitudes E^+ and E^- in each layer and subsequently T_{cal} and R_{cal} can be connected by the TM method.

The electric fields at both sides of each interface are defined by

$$\begin{pmatrix} E_m^+ \\ E_m^- \end{pmatrix} = \mathbf{M}_{m,m+1} \begin{pmatrix} E_{m+1}^+ \\ E_{m+1}^- \end{pmatrix}, \tag{3}$$

where $\mathbf{M}_{m,m+1} = \dfrac{1}{t_{m,m+1}} \begin{pmatrix} 1 & r_{m,m+1} \\ r_{m,m+1} & 1 \end{pmatrix}.$ (4)

$t_{m,m+1}$ and $r_{m,m+1}$ are the transmission and reflection Fresnel coefficient, respectively, and they are a function of the complex refractive index of the media forming the interface.

The electric fields at the left and right side of the mth layer are related by

$$\begin{pmatrix} E_{m1}^+ \\ E_{m1}^- \end{pmatrix} = \boldsymbol{D_m} \begin{pmatrix} E_{m2}^+ \\ E_{m2}^- \end{pmatrix}, \tag{5}$$

where $\boldsymbol{D_m} = \begin{pmatrix} e^{-i\theta_m} & 0 \\ 0 & e^{i\theta_m} \end{pmatrix}.$ (6)

θ_m is the phase shift of light propagating through the mth layer, and is given by $\theta_m = 2\pi N_m d_m / \lambda$. N_m and d_m are the complex refractive index and the thickness of the mth layer, respectively. For our case, we could apply the matrix transformations deduced above to connect the electric field amplitudes E_a and E_d

$$\begin{pmatrix} E_a^+ \\ E_a^- \end{pmatrix} = \boldsymbol{M}_{a,b} \boldsymbol{D}_b \boldsymbol{M}_{b,c} \boldsymbol{D}_c \boldsymbol{M}_{c,d} \begin{pmatrix} E_d^+ \\ 0 \end{pmatrix}$$
$$= \begin{pmatrix} T_{11} & T_{12} \\ T_{21} & T_{22} \end{pmatrix} \boldsymbol{D}_c \boldsymbol{M}_{c,d} \begin{pmatrix} E_d^+ \\ 0 \end{pmatrix}. \tag{7}$$
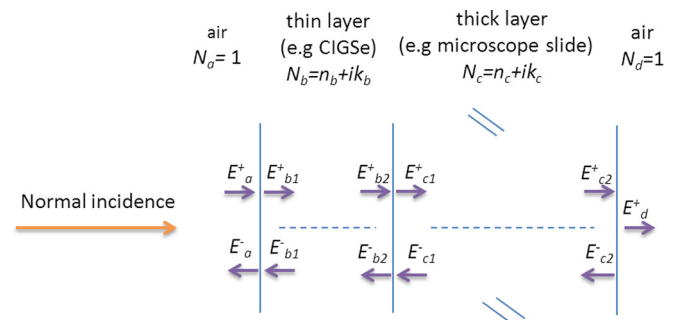

FIG. 1. Schematic of the stacked structure for the determination of optical constants.

In order to deal with coherent propagation within thin films and incoherent propagation through thick substrates, Harbecke proposed to decompose the layer structure into thin and thick sub-layer structures, then square the electric field amplitude separately.[20] The relationship of the incident (I_{in}), the reflected (I_r), and the transmitted (I_t) light intensity for our experimental layer structure can be finally gained as follows:

$$\begin{pmatrix} I_{in} \\ I_r \end{pmatrix} = |T_{11}|^2 \begin{pmatrix} 1 & -\left|\frac{T_{12}}{T_{11}}\right|^2 \\ \left|\frac{T_{21}}{T_{11}}\right|^2 & \left|\frac{T_{11}T_{22}-T_{21}T_{12}}{T_{11}}\right|^2 - \left|\frac{-T_{21}T_{12}}{(T_{11})^2}\right|^2 \end{pmatrix} \begin{pmatrix} |e^{-i\theta_b}|^2 & 0 \\ 0 & |e^{i\theta_b}|^2 \end{pmatrix} \begin{pmatrix} \dfrac{1}{|t_{c,d}|^2} & -\dfrac{|r_{d,c}|^2}{|t_{c,d}|^2} \\ \dfrac{|r_{c,d}|^2}{|t_{c,d}|^2} & \dfrac{|t_{c,d}t_{d,c}|^2 - |r_{c,d}r_{d,c}|^2}{|t_{c,d}|^2} \end{pmatrix} \begin{pmatrix} I_t \\ 0 \end{pmatrix}$$

$$= \begin{pmatrix} S_{11} & S_{12} \\ S_{21} & S_{22} \end{pmatrix} \begin{pmatrix} I_t \\ 0 \end{pmatrix}. \tag{8}$$

So it is easy to derive the analytical expressions of T_{cal} and R_{cal}

$$R_{cal} = \frac{S_{21}}{S_{11}}, \tag{9}$$

$$T_{cal} = \frac{1}{S_{11}}. \tag{10}$$

2. MTM method

However, the TM method could not treat the partially coherent propagation of light (scattered part), which usually results from interface roughness. In order to take the interface roughness into account and consider the influence of scattered light, the TM method was modified by introducing the modified Fresnel coefficients (abbreviated as MTM method)[14]

$$r'_{a,b} = r_{a,b} \exp[-2(2\pi\sigma/\lambda)^2 n_a^2], \tag{11}$$

$$r'_{b,a} = r_{b,a} \exp[-2(2\pi\sigma/\lambda)^2 n_b^2], \tag{12}$$

$$t'_{a,b} = t_{a,b} \exp\left[-\left(\frac{2\pi\sigma}{\lambda}\right)^2 (n_a - n_b)^2/2\right], \tag{13}$$

$$t'_{b,a} = t_{b,a} \exp\left[-\left(\frac{2\pi\sigma}{\lambda}\right)^2 (n_a - n_b)^2/2\right]. \tag{14}$$

Here, σ is the surface roughness in terms of root mean square (RMS) value, and $r'_{a,b}$, $r'_{b,a}$, $t'_{a,b}$, and $t'_{b,a}$ denote the corresponding modified Fresnel coefficients. It should be noted here that only the roughness at the interface between air and the CIGSe film is taken into account for our case, because the scattering effect of the interface between the substrate and the CIGSe film is neglected due to the relatively smooth surface of the microscope slide. Since the MTM method can establish the relationship of the specular components $R_{spe}(\lambda)$ and $T_{spe}(\lambda)$ on real films to the corresponding $R_{tot}(\lambda)$ and $T_{tot}(\lambda)$ on ideally flat films by introducing the modified Fresnel coefficients, $R_{tot}(\lambda)$ and $T_{tot}(\lambda)$ are substituted by the specular components on real films. Subsequently, Eqs. (1) and (2) evolve to

$$R'_{cal}(n_b(\lambda), k_b(\lambda)) - R_{spe}(\lambda) = 0, \tag{15}$$

$$T'_{cal}(n_b(\lambda), k_b(\lambda)) - T_{spe}(\lambda) = 0. \tag{16}$$

$R'_{cal}(\lambda)$ and $T'_{cal}(\lambda)$ are the analytical expressions of reflectance and transmittance after introducing the modified Fresnel coefficients in Eqs. (11)–(14).

A program based on the equations above was developed via the software WOLFRAM MATHEMATICA and enables to calculate (n_b, k_b) data for each wavelength and extract the physically meaningful optical constants from multiple solutions.

III. RESULTS AND DISCUSSION

Fig. 2 compares the top view of CGSe and CISe before and after smoothening. Images taken with SEM and AFM both show that the surface of CGSe and CISe was smoothened after etching with bromine solution. The surface roughness (RMS) σ was reduced from 9 nm to 3 nm for CGSe and from 20 nm to 10 nm for CISe. These smoothened samples will be used as references and to verify that the MTM method can improve the accuracy of the computation of optical constants in the following.

In Figs. 3(a) and 3(b), we can see that the interference fringes of R_{tot} after etching shift for both samples. This is attributed to the fact that the bromine solution can reduce the thickness of the films as well (from 300 to 265 nm for CGSe and 270 to 158 nm for CISe) while smoothing the surface in our samples.[17] Above the bandgap ($\lambda < 1230$ nm for CISe and <730 nm for CGSe), the interference amplitude gradually shrinks with decreasing the wavelength, which results from destructive effects of absorption and surface scattering. After smoothening, R_{tot} of both CGSe and CISe increases overall in the short wavelength, especially for CISe where the absolute reduction of surface roughness is bigger. At the same time, R_{dif} of CISe drops sharply after smoothening, but is still relatively large. For the sample CGSe, R_{dif} is negligible compared to that of CISe due to the relatively smaller surface roughness. R_{dif} stems from the surface scattering and
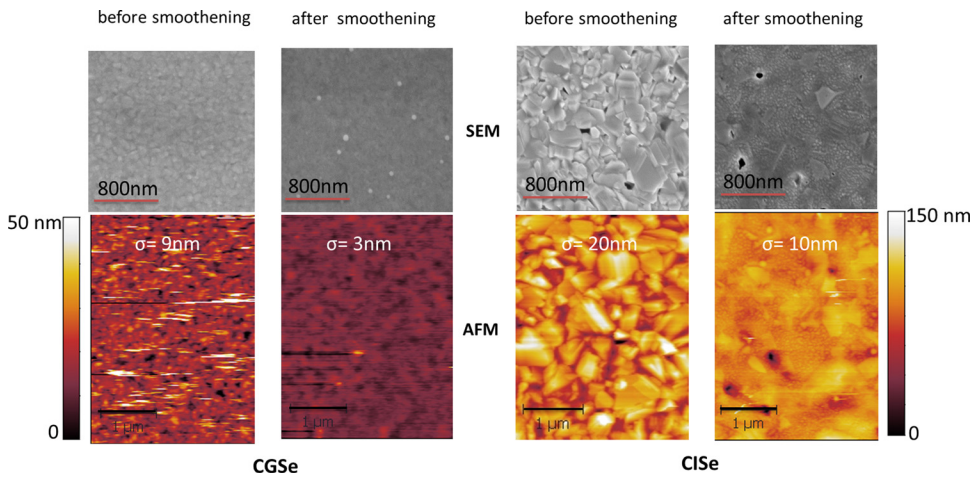
FIG. 2. Top views of samples CGSe and CISe both before and after smoothening.

is closely related to the surface roughness. After smoothening, the surface roughness is reduced, which is confirmed by Fig. 2. The reduced surface roughness can then weaken the scattering of light, which is in accordance with the drop of R_{dif} of CISe in Fig. 3.

In Figs. 3(c) and 3(d), the curves of computed refractive index values for CGSe and CISe are presented: multiple n solutions (expressed in the symbol of $\tilde{n}$) are observed. To begin with, we should stress that the existence of multiple solutions, which originates from the nature of the complex implicit equations (Eqs. (1) and (2)), is the main disadvantage of the TM method. In addition, the reflectance (R) is more sensitive to the surface roughness than the transmittance (T) and the multiplicity of solutions for n is more complicated in contrast to that of the absorption coefficient (k).Therefore, R and n are mainly taken to illustrate the effect of the surface roughness.

Taking the multiple n solution curves of $\tilde{n}_{TM}^{Rou}$, calculated with the TM method without considering surface roughness for the two samples before smoothening, as examples, one feature can be observed: the multiplicity of solutions forms solution branches. Theoretically, the solution branches should coincide tangentially and form a continuous dispersion curve, which the physically meaningful values correspond to.[10] However, the adjacent solution branches fail to be in good tangency, and discontinuities (called branch gaps) appear especially in the short wavelength range. This signifies that no physically meaningful value can be found at the branch gaps. Besides, the branch gaps tend to widen with decreasing wavelength. There are many factors in the experiments, which reduce the applicability of the TM method to the practical situation and thus lead to the occurrence of branch gaps.[9,10] Among these factors, the main one is related to the scattering of light from rough surfaces, which leads to
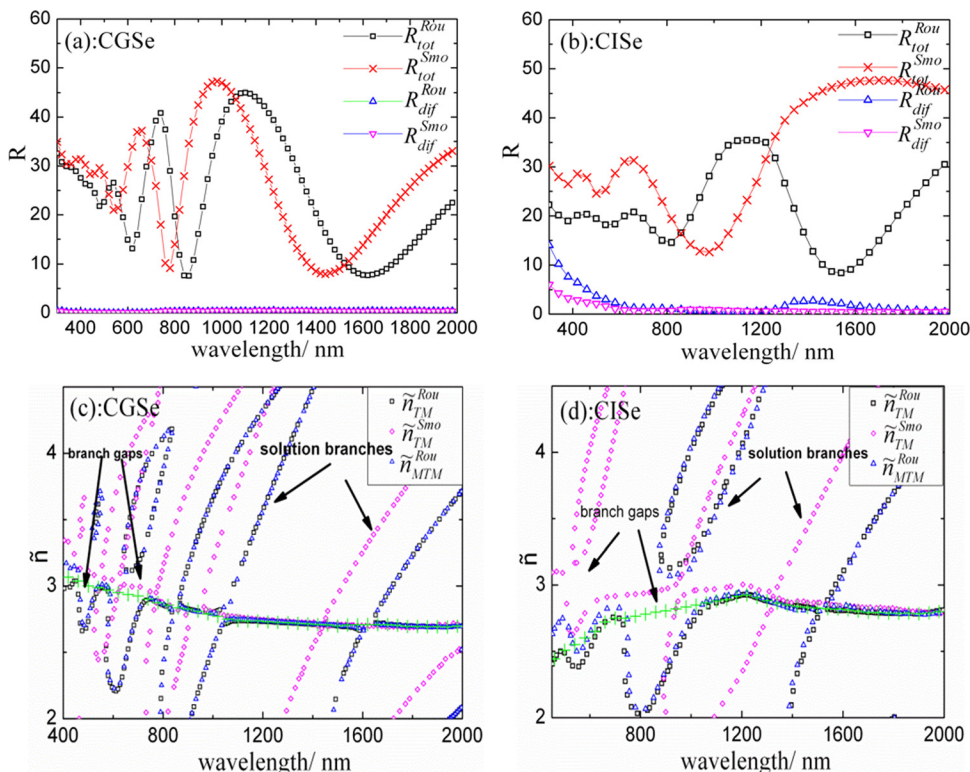

FIG. 3. Total (R_{tot}) and diffuse (R_{dif}) reflectance of samples (a) CGSe and (b) CISe, multiple solutions ($\tilde{n}$) of refractive index of (c) CGSe and (d) CISe both before and after smoothening. Superscripts "Rou" and "Smo" correspond to that the measurement (R) or the calculation ($\tilde{n}$) is done for the samples before smoothening and after smoothening, respectively. $\tilde{n}_{TM}$ indicates that the multiple n solutions are calculated by the TM method without considering surface roughness and $\tilde{n}_{MTM}$ that the MTM method considering surface roughness was applied. The green cross-dotted lines in Figs. 3(c) and 3(d) mark the physically meaningful values selected out of the multiple solution curves $\tilde{n}_{TM}^{Rou}$ from CGSe and CISe, respectively.
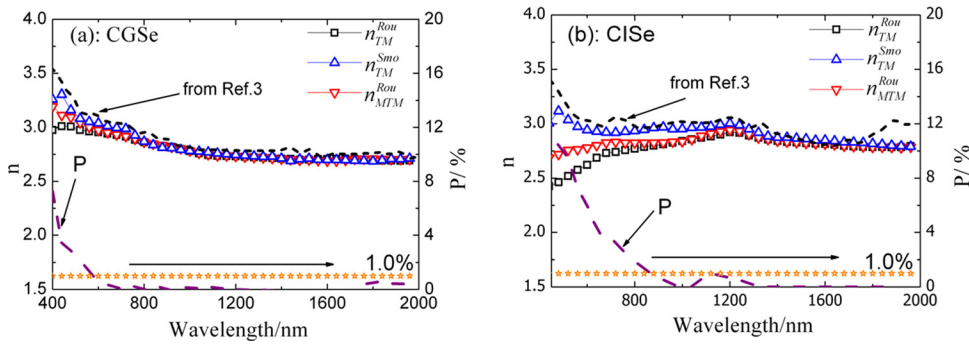
FIG. 4. Physically meaningful n data of CGSe (a) and CISe (b) extracted from corresponding curves in Figs. 3(c) and 3(d), respectively (n_{TM}^{Rou} originates from $\tilde{n}_{TM}^{Rou}$ and likewise for the rest). The dotted line corresponds that the values are from Orgassa in Ref. 3. P denotes $\frac{n_{MTM}^{Rou}-n_{TM}^{Rou}}{n_{TM}^{Rou}}$. P, less than 1%, is regarded as the experimental error.

interference shrinkage and intensity reduction of R/T compared to smooth surfaces.[13,16,18,21] The CIGSe films exhibit a certain surface roughness (Fig. 2), and the scattering exists. But the TM method requires the interfaces in the layer structure to be perfectly flat and there is no scattering. Therefore, for the practically measured R/T, the TM method is less applicable. The calculated optical constants then deviate from inherent values, solution branches fail to coincide tangentially, and branch gaps form.

The scattering effect is consistent with surface roughness and more pronounced with decreasing wavelength. For high surface roughness, in the short wavelength range, the measured R/T will deviate more from the ideal values on the flat surface. Thereby the branch gaps in solution curves $\tilde{n}_{TM}^{Rou}$ from both samples tend to widen as the wavelength decreases. Besides, the curve $\tilde{n}_{TM}^{Rou}$ from CISe exhibits wider branch gaps than that from CGSe due to the higher surface roughness of CISe compared to CGSe.

To reduce the negative effect of surface roughness on the calculation of optical constants, both CGSe and CISe were smoothened. The TM method is expected to suit the smoothened samples much better due to the much smaller effect of scattering. Multiple n solution curves for each smoothened sample $\tilde{n}_{TM}^{Smo}$ are also shown in Figs. 3(c) and 3(d). Comparing the curve $\tilde{n}_{TM}^{Smo}$ (after smoothening) to $\tilde{n}_{TM}^{Rou}$ (before smoothening) for each sample clearly shows that the results are in agreement with our theoretical analysis. The continuity improves for the calculations of both smoothened samples: branch gaps largely narrow or even disappear. For the smoothened CGSe with very low surface roughness ($\sigma = 3$ nm), the scattering effect is negligible. However, the branch gaps in $\tilde{n}_{TM}^{Smo}$ still exist. It should be noted that it is of extreme difficulty to get a completely continuous curve without any tiny branch gaps even for a perfectly smooth sample. This is because any uncertainties, such as voids within the film,[22] thickness inhomogeneity,[10] a thin oxide layer on the surface,[9] the measured error of the thickness,[14] imperfect monochromaticity[23] of measured incident light, can reduce the applicability of the TM method and lead to branch gaps as well.

As stated theoretically above, the MTM method can compensate for the effect of surface roughness directly without smoothening the samples. The MTM method was applied for the samples CGSe and CISe without smoothening. The multiple solution n curves ($\tilde{n}_{MTM}^{Rou}$) are illustrated in Figs. 3(c) and 3(d) as well. It can be clearly observed for each sample that the continuity of the curve $\tilde{n}_{MTM}^{Rou}$ (considering roughness) also improves in contrast to $\tilde{n}_{TM}^{Rou}$ (not

considering roughness). This is due to the fact that the σ/λ factor in the MTM method considers the surface roughness-induced scattering. However, the continuity of $\tilde{n}_{MTM}^{Rou}$ fails to go to the extent that $\tilde{n}_{TM}^{Smo}$ curves from smoothened samples can reach. This implies that the MTM method can only partially consider for the effect of surface roughness. To explain this point, we should go back to the theory and re-check the validation assumptions of the MTM method.[14] Among them, the surface roughness σ should be much smaller compared to the wavelength of incident light λ ($\sigma/\lambda \ll 1$). When this requirement is not completely fulfilled, the effect of multiple reflection[24] will become stronger and the MTM method will fail to fully calibrate measured R/T.

For quantitative illustration of the changes of n values after applying the MTM method to the rough samples and the TM method to the smoothened samples compared to the application of the TM method to the rough samples, the physically meaningful n values from all $\tilde{n}$ curves were extracted and are shown in Fig. 4. The solution branches should form a continuous line (physically meaningful n curve) around $n = 3$ for ideally smooth CISe and CGSe; for practical samples with surface roughness, branch gaps exist in the short wavelength range and a spline function[3] was used to deal with the branch gaps of multiple n solution curves (for more details about the selecting criteria and related, see Ref. 3). Two cross-dotted lines in Figs. 3(c) and 3(d) are shown as examples for the physically meaningful n curves extracted from the multiple solution curve $\tilde{n}_{TM}^{Rou}$ for each sample (To avoid confusion, only the two exemplary n curves are presented in Figs. 3(c) and 3(d)).

In Fig. 4, physically meaningful n curves were extracted from all multiple solution curves $\tilde{n}$ in Fig. 3. The physically meaningful curve n_{TM}^{Rou} results from the multiple solution curve $\tilde{n}_{TM}^{Rou}$ and likewise for the rest. $\tilde{n}_{TM}^{Smo}$ was calculated from smoothened sample and has the highest continuity among all multiple solution curves for each sample. The corresponding extracted n values (n_{TM}^{Smo}) are thus regarded most comparable to the inherent values. In the following, n_{TM}^{Smo} are approximately considered as the inherent values and will serve as the standard values. From Fig. 4, we can see that the curve n_{MTM}^{Rou} increases in the short wavelength range and approaches n_{TM}^{Smo} further compared to n_{TM}^{Rou} for each sample. This implies that the MTM method can improve the accuracy of the calculation and partially calibrate the effect of surface scattering.

P, given as $\frac{n_{MTM}^{Rou}-n_{TM}^{Rou}}{n_{TM}^{Rou}}$, is used to quantify the increased amplitude of the n value after applying the MTM method for

both samples. The increased amplitude declines gradually as the wavelength increases in both P curves. Additionally, the overall increased amplitude (average of $\sum P$ over the wavelength range where P > 1%) is much lower for CGSe (2.59%) than for CISe (6.89%), in general. This is due to the fact that the σ/λ factor in the modified Fresnel coefficients can increase the corrected R and the increased amplitude proportionally depends on σ/λ.[14] As it was proven both in our simulation and in literature,[10] higher R indicates higher n value; higher roughness value introduced in the MTM method can thus result in higher increased amplitude of n value.

AFM images in Fig. 2 show that the surface roughness of CISe ($\sigma = 20$ nm) is much higher than that of CGSe ($\sigma = 10$ nm). The increase of the n value of CISe (P for CISe) is thus bigger than that of CGSe (P for CGSe) after applying the MTM method. As the wavelength keeps increasing, the factor σ/λ decreases with it. Therefore, the increasing effect for n brought by the factor σ/λ will be gradually reduced. This agrees with the changing trend of both P curves (for P < 1%, the change is regarded as experimental error).

For comparison, the refractive indexes of CISe and CGSe from Orgassa[3] are displayed in Fig. 4 as well. These data were also calculated by the MT method without taking surface roughness into account. As can be seen, the refractive indexes from Orgassa are generally a little higher than our values but still in good agreement. The observed discrepancy is most likely to stem from the samples themselves. This is because the morphology and structure of CIGSe thin films are very sensitive to preparation parameters and thus the optical constants possibly change as well. Besides, the discrepancy implies that it is of crucial importance to obtain the practical optical constants of the samples for further accurate application. Nevertheless, we stress more the surface roughness model to obtain more accurate optical constants than the calculated values themselves in this paper.

As we stated above, the MTM method can partially compensate for the effect of surface roughness. To illustrate the degree of the improvement of the MTM method for both CGSe and CISe, n_{MTM}^{Rou} values need to be compared to the inherent values. Inherent values are replaced by n_{TM}^{Smo} values due to the high comparability we analyzed above. We define the conformity ratio G to describe the degree of improvement. G denotes the average value of $\sum \frac{n_{MTM}^{Rou}}{n_{TM}^{Smo}}$ above the bandgap since the obvious difference locates mainly in this spectrum range. Obviously, a higher G value implies higher conformity to the inherent values. It is calculated that the G value for CGSe (G = 0.979) is higher than that for CISe (G = 0.954). As can be obviously seen in Fig. 4, n_{MTM}^{Rou} values for CGSe approach to the corresponding n_{TM}^{Smo} values much closer than CISe, which indicates that the MTM method is applicable much better for CGSe with low surface roughness than for CISe with high surface roughness. This is in accordance with the assumption of $\sigma/\lambda \ll 1$ stated above. CGSe is more in line with the assumption than CISe, thereby the conformity factor G for CGSe is higher.

IV. CONCLUSION

In this paper, optical constants of CISe and CGSe were calculated by applying the TM or the MTM method to macroscopic optical measurements of R/T. The MTM method was proposed to calculate the optical constants taking surface roughness into account and compared to the TM method without taking surface roughness into account. For both CISe and CGSe, it was discovered that the MTM method could improve the continuity of the multiple-solution n curves and enhance the accuracy of the calculation. In contrast to the optical constants from relatively smooth CGSe and CISe, the MTM method was proven to be effective in considering the influence of surface roughness for both samples and has better applicability for CGSe with low surface roughness than CISe with high surface roughness.

[1]A. Jager-Waldau, Sol. Energy Mater. Sol. Cells **95**, 1509 (2011).
[2]P. Jackson, D. Hariskos, E. Lotter, S. Paetel, R. Wuerz, R. Menner, W. Wischmann, and M. Powalla, Prog. Photovoltaics **19**, 894 (2011).
[3]K. Orgassa, Ph.D. dissertation, University of Stuttgart, 2004.
[4]M. Schmid, J. Krč, R. Klenk, M. Topič, and M. C. Lux-Steiner, Appl. Phys. Lett. **94**, 053507 (2009).
[5]A. B. Djurisic and E. H. Li, Appl. Phys. A **73**, 189 (2001).
[6]M. I. Alonso, M. Garriga, C. A. D. Rinc, and E. Hern, Appl. Phys. A **74**, 659 (2002).
[7]M. Alonso, K. Wakita, J. Pascual, M. Garriga, and N. Yamamoto, Phys. Rev. B **63**, 075203-1 (2001).
[8]S. Theodoropoulou, D. Papadimitriou, C. Anestou, C. Cobet, and N. Esser, Semicond. Sci. Technol. **24**, 015014 (2009).
[9]R. E. Denton, R. D. Campbell, and S. G. Tomlin, J. Phys. D: Appl. Phys. **5**, 852 (1972).
[10]P. O. Nilsson, Appl. Opt. **7**, 435–442 (1968).
[11]O. Lundberg, M. Bodegard, J. Malmstrom, and L. Stolt, Prog. Photovoltaics **11**, 77 (2003).
[12]N. Barreau, J. Lähnemann, F. Couzinié-Devy, L. Assmann, P. Bertoncini, and J. Kessler, Sol. Energy Mater. Sol. Cells **93**, 2013 (2009).
[13]M. Schmid, R. Klenk, and M. C. Lux-Steiner, Sol. Energy Mater. Sol. Cells **93**, 874 (2009).
[14]J. Szczyrbowski, J. Phys. D: Appl. Phys. **11**, 583 (1978).
[15]E. Centurioni, Appl. Opt. **44**, 7532–7539 (2005).
[16]C. C. Katsidis and D. I. Siapkas, Appl. Opt. **41**, 3978 (2002).
[17]M. Bouttemy, P. Tran-Van, I. Gerard, T. Hildebrandt, A. Causier, J. L. Pelouard, G. Dagher, Z. Jehl, N. Naghavi, G. Voorwinden, B. Dimmler, M. Powalla, J. F. Guillemoles, D. Lincot, and A. Etcheberry, Thin Solid Films **519**, 7207 (2011).
[18]M. C. Troparevsky, A. S. Sabau, A. R. Lupini, and Z. Zhang, Opt. Express **18**, 24715–24721 (2010).
[19]K. Ohta and H. Ishida, Appl. Opt. **29**, 1952 (1990).
[20]B. Harbecke, Appl. Phys. B **39**, 165 (1986).
[21]C. L. Mitsas and D. I. Siapkas, Appl. Opt. **34**, 1678 (1995).
[22]M. Vanecek, J. Holoubek, and A. Shah, Appl. Phys. Lett. **59**, 2237 (1991).
[23]R. Swanepoel, J. Phys. E: Sci. Instrum. **16**, 1214 (1983).
[24]H. E. Bennett and J. O. Porteus, J. Opt. Soc. Am. **51**, 123 (1961).